Report

Cell Reports

Simple and Rapid In Vivo Generation of Chromosomal Rearrangements using CRISPR/Cas9 Technology

Graphical Abstract

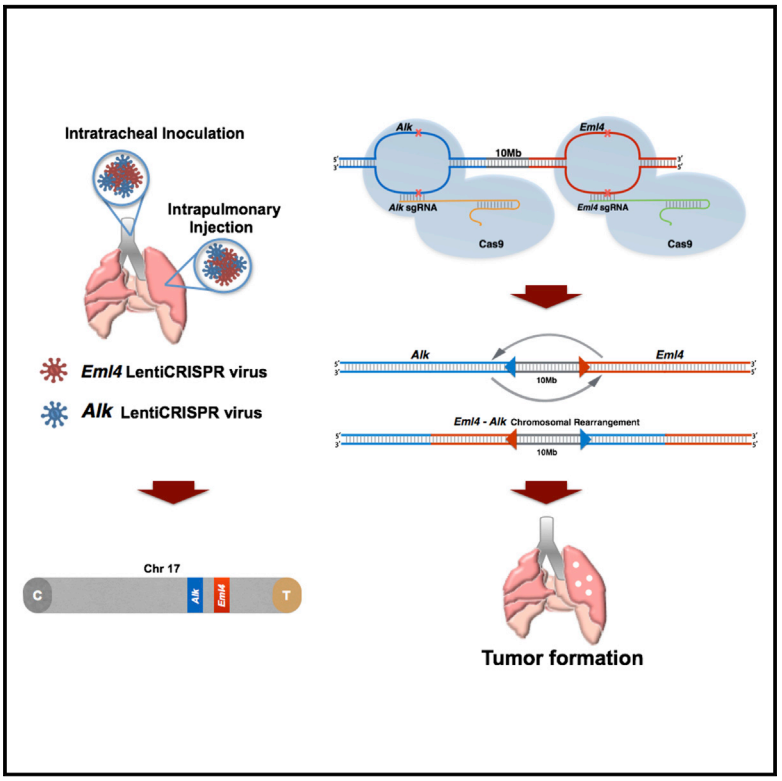

Highlights

CRISPR/Cas9 technology is exploited to generate *Eml4-Alk* rearrangements in vitro

Eml4-Alk rearrangements are obtained in vivo and induce tumor formation in mice

Additional chromosomal rearrangements are generated as a result of the induced DSBs

Authors

Rafael B. Blasco, Elif Karaca, ..., Claudia Voena, Roberto Chiarle

Correspondence

roberto.chiarle@childrens.harvard.edu

In Brief

Blasco et al. demonstrate that CRISPR/Cas9 technology can be exploited to generate targeted chromosomal rearrangements in vivo in mice in a time- and cost-effective approach.

Blasco et al., 2014, Cell Reports 9, 1219–1227
November 20, 2014 ©2014 The Authors
http://dx.doi.org/10.1016/j.celrep.2014.10.051

Cell Reports
Report

Simple and Rapid In Vivo Generation of Chromosomal Rearrangements using CRISPR/Cas9 Technology

Rafael B. Blasco,[1,4] Elif Karaca,[1,4] Chiara Ambrogio,[2] Taek-Chin Cheong,[1] Emre Karayol,[1] Valerio G. Minero,[3] Claudia Voena,[1,3] and Roberto Chiarle[1,3,*]
[1]Department of Pathology, Boston Children's Hospital and Harvard Medical School, Boston, MA 02115, USA
[2]Molecular Oncology Program, Centro Nacional de Investigaciones Oncológicas, 28029 Madrid, Spain
[3]Department of Molecular Biotechnology and Health Sciences, University of Torino, 10126 Torino, Italy
[4]Co-first author
*Correspondence: roberto.chiarle@childrens.harvard.edu
http://dx.doi.org/10.1016/j.celrep.2014.10.051

SUMMARY

Generation of genetically engineered mouse models (GEMMs) for chromosomal translocations in the endogenous loci by a knockin strategy is lengthy and costly. The CRISPR/Cas9 system provides an innovative and flexible approach for genome engineering of genomic loci in vitro and in vivo. Here, we report the use of the CRISPR/Cas9 system for engineering a specific chromosomal translocation in adult mice in vivo. We designed CRISPR/Cas9 lentiviral vectors to induce cleavage of the murine endogenous *Eml4* and *Alk* loci in order to generate the *Eml4-Alk* gene rearrangement recurrently found in non-small-cell lung cancers (NSCLCs). Intratracheal or intrapulmonary inoculation of lentiviruses induced *Eml4-Alk* gene rearrangement in lung cells in vivo. Genomic and mRNA sequencing confirmed the genome editing and the production of the *Eml4-Alk* fusion transcript. All mice developed *Eml4-Alk*-rearranged lung tumors 2 months after the inoculation, demonstrating that the CRISPR/Cas9 system is a feasible and simple method for the generation of chromosomal rearrangements in vivo.

INTRODUCTION

Chromosomal rearrangements are key causative events in several types of human cancers (Gostissa et al., 2011; Mitelman et al., 2007). The generation of genetically engineered mouse models (GEMMs) that faithfully recapitulate chromosomal rearrangements have been instrumental to advance the understanding of the biology and therapy of cancer (Rabbitts et al., 2001). However, design and generation of GEMMs for chromosomal rearrangements targeted in the endogenous loci is expensive and time consuming. The bacterial type II clustered regularly interspaced short palindromic repeat (CRISPR)/CRISPR-associated (Cas) systems have recently shown great potential for RNA-guided genome editing, including multiplexing genome engineering (Cong et al., 2013; Mali et al., 2013), homologous recombination and gene targeting (Wang et al., 2013; Yang et al., 2013), and regulation of transcription (Gilbert et al., 2013). CRISPR/Cas9 systems have been successfully used for precise genome editing in mouse embryonic stem cells (ESCs) and targeted biallelic mutagenesis in F0 zebrafish (Jao et al., 2013; Wang et al., 2013; Yang et al., 2013). Recently, CRISPR-Cas9 systems have been used to efficiently edit the genome of adult mice in vivo in liver and muscle (Long et al., 2014; Xue et al., 2014; Yin et al., 2014).

The RNA-guided Cas9 endonuclease induces sequence-specific DNA double-strand breaks (DSBs) that are repaired mostly by the classical and alternative nonhomologous end-joining pathways (c-NHEJ or AEJ) or by homology-directed repair (HDR) (Boboila et al., 2012). The DSB repair mediated by end-joining pathways can lead to insertion/deletion (indel) mutations, but it can also be inappropriately resolved into a chromosomal rearrangement (Alt et al., 2013; Chiarle et al., 2011; Klein et al., 2011). During the last few years, several studies demonstrated that DSBs generated by genome editing tools like zinc-finger nucleases (ZFNs) and transcription activator-like effector nucleases (TALENs) can be resolved into chromosomal rearrangements in human cell lines (Brunet et al., 2009; Lee et al., 2012; Piganeau et al., 2013) and zebrafish (Gupta et al., 2013; Xiao et al., 2013). Similarly, recent reports in cell lines in vitro demonstrated the potential application of the CRISPR/Cas9 system to induce, at high frequency, targeted cancer-associated chromosomal rearrangements in human cell lines, such as *EML4-ALK*, *CD74-ROS1*, *KIF5B-RET*, *EWSR1-FLI1*, and *AML1-ETO* rearrangements, by designing pairs of specific guide RNAs for the loci of interest (Choi and Meyerson, 2014; Torres et al., 2014).

EML4-ALK rearrangement is found in about 5%–7% of non-small-cell lung cancers (NSCLCs) and is one of the most frequent rearrangements in solid human cancers (Chiarle et al., 2008; Soda et al., 2007). In NSCLC, the *EML4-ALK* rearrangement is generated by an inversion of a chromosomal segment of ~12 Mb on human chromosome 2 with breakpoints in intron 19 of the human *ALK* gene and variable breakpoints in the *EML4* gene, the most frequent being in intron 13 (Mano, 2008). This chromosomal inversion generates an EML4-ALK fusion protein

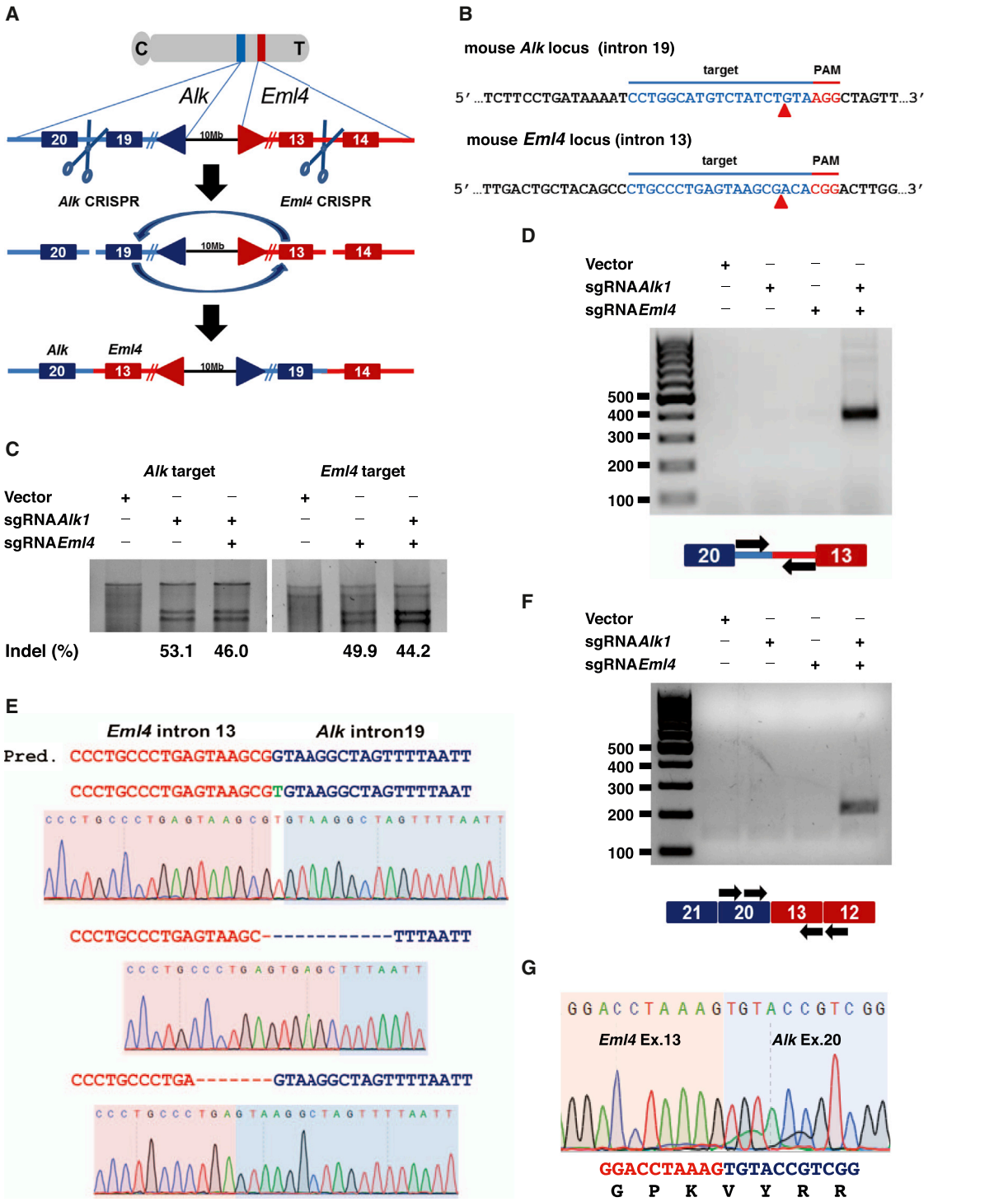

Figure 1. Generation of *Eml4-Alk* Rearrangements by the CRISPR/Cas9 System in Mouse Cells In Vitro

(A) Schematic representation of the CRISPR/Cas9-generated DSBs in the intron 19 of the *Alk* locus and in intron 13 of the *Eml4* locus. Simultaneous generation of DSBs induces a chromosomal inversion of ~10 Mb, leading to the generation of the *Eml4-Alk* chromosomal rearrangement.

(B) Schematic representation of base pairing between *Alk* and *Eml4* genomic loci and targeting sgRNAs. Red arrow indicates putative cleavage site.

(C) SURVEYOR assay for CRISPR/Cas9-mediated indels in the *Alk* and *Eml4* genomic loci.

(D) Detection of *Eml4-Alk* rearrangements by PCR on genomic DNA extracted from ASB-XIV lung cell line transduced with lentivirus expressing the Cas9 nuclease (vector) alone or together with Eml4 or Alk sgRNA. Black arrows indicate PCR primers designed in intron 19 of the *Alk* locus and intron 13 of the *Eml4* locus.

(legend continued on next page)

that has constitutive tyrosine kinase activity that drives NSCLC growth (Chiarle et al., 2008; Shaw and Engelman, 2013).

In this study, we show the CRISPR/Cas9 system can be exploited to directly engineer *Eml4-Alk* rearrangements in vivo in adult mice. As a consequence of *Eml4-Alk* rearrangement induction, mice developed lung tumors within a short period of time. Therefore, this approach represents a simple and cost-effective method to model chromosomal rearrangements that could be used as an alternative to classical transgenic or knockin mice for a variety of biological and cancer studies.

RESULTS

Generation of *Eml4-Alk* Rearrangements and *Eml4-Alk* Fusion mRNA In Vitro by the CRISPR/Cas9 System

We engineered lentiviral vectors expressing Cas9 endonuclease and single-guide RNA (sgRNA) specific for either the *Eml4* or the *Alk* mouse genomic locus. As the mouse *Eml4* gene has a noncoding exon 1, which is lacking in human *EML4*, we designed sgRNAs to target intron 14 of the mouse *Eml4* gene, which is the equivalent of intron 13 of the human *EML4* gene. However, for parallelism with the human EML4-ALK rearrangement in NSCLC, in this paper, we will refer to this as intron 13. In the mouse *Alk* gene, the sgRNAs were designed to target intron 19 as in human EML4-ALK rearrangements, in order to generate DSBs in that position and eventually obtain a chromosomal breakpoint comparable to those found in human NSCLC (Figures 1A and 1B). Out of several independent sgRNAs, we selected the most efficient sequences by SURVEYOR assay for further use (Cong et al., 2013) (Figure 1C).

Next, we tested whether the combination of the two lentiviruses encoding *Eml4* and *Alk* sgRNAs would induce *Eml4-Alk* rearrangements at detectable frequency in murine cells. We transduced either murine immortalized tail fibroblasts or a murine lung carcinoma cell line (ASB-XIV) with single or both lentiviruses. Six days after transduction, the genomic product corresponding to the *Eml4-Alk* rearrangement was readily detectable in both cell types only when both *Eml4* and *Alk* sgRNA lentiviruses were used (Figures 1D and S1A). We Sanger sequenced several independent genomic breakpoint junctions to show that the CRISPR/Cas9 system can generate either precise genomic junctions originated by direct repair of the predicted DNA cleavage sites (three bases on the 5′ end of the PAM sequence) or junctions with base insertions or deletions, a process consistent with editing by NHEJ (Alt et al., 2013) (Figure 1E). As predicted by the genomic breakpoint, such engineered *Eml4-Alk* rearrangements should produce in-frame fusion *Eml4-Alk* mRNA transcripts joining coding exons 1–13 of the *Eml4* gene and exons 20–29 of the *Alk* gene. Indeed, we detected in both cell lines mRNA fusion transcripts encoding for an in-frame EML4-ALK chimeric protein identical to that found in human NSCLC (Figures 1F, 1G, and S1B). Thus, the CRISPR/Cas9 system can efficiently generate the desired chromosomal rearrangement by introducing DSBs in the targeted sites.

Other chromosomal events could be predicted as the result of the simultaneous activity of CRISPR/Cas9 on the *Eml4* and *Alk* loci located on the two alleles of chromosome 17. It is well known that DSBs generated by nucleases located in *cis* on the same chromosomal allele can result in deletions of the chromosome portion between the two DSBs in the immunoglobulin H (IgH) locus (Zarrin et al., 2007) as well as in other genomic loci (Gostissa et al., 2014). This general propensity of intrachromosomal DSBs to be frequently joined, even at long distances, could be the result of the nuclear architecture of chromosomal territories (Hakim et al., 2012; Zhang et al., 2012). Thus, we investigated whether intrachromosomal deletions were generated by the simultaneous activity of CRISPR/Cas9 on the *Eml4* and *Alk* genes (Figure S1C). Indeed, in both fibroblast and lung cells, we found genomic junctions that corresponded to a deletion of the 10 Mb region between the *Eml4* and *Alk* on chromosome 17 (Figure S2A). In addition to deletions, other complex chromosomal rearrangements could be also predicted, including the formation of dicentric or acentric chromosomes, when DSBs on both alleles of the *Eml4* or the *Alk* locus are joined (Figure S1C). However, we did not detect such rearrangements by PCR, indicating that they could be rare or alternatively be lost during cell replication because genetically unstable. Finally, we found genomic junctions between the intron 13 of *Eml4* and intron 19 of *Alk* (Figure S2B). These could be explained either as large 10 Mb deletion circles (Figure S1C) or as interchromosomal translocations with duplication of the 10 Mb region between the *Eml4* and the *Alk* loci (Figure S1C). Therefore, we concluded that engineering the genome with CRISPR/Cas9 system in two independent loci leads to several genomic rearrangements that can be predicted by the position of the targeted loci.

Generation of *Eml4-Alk* Rearrangements and *Eml4-Alk* Fusion mRNA In Vivo by the CRISPR/Cas9 System

Next, we tested whether *Eml4-Alk* rearrangements could be obtained in vivo in adult mice. Since *Eml4-Alk* rearrangements are mostly found in human NSCLC, we delivered lentiviral particles to lungs of adult mice either by intratracheal inoculation (Simpson et al., 2001) or by direct intrapulmonary injection (Onn et al., 2003) (Figure 2A). We inoculated mice with both lentiviruses expressing Cas9/*Alk* sgRNA and Cas9/*Eml4* sgRNA. As controls, we inoculated mice with lentiviruses expressing Cas9 without sgRNA or expressing *Eml4 sgRNA* or *Alk* sgRNA alone. After 6 days of lentiviral inoculation, we took the lungs for DNA isolation in order to investigate the presence of *Eml4-Alk* rearrangements by PCR and sequencing. Following intratracheal inoculation or intrapulmonary injections, we detected *Eml4-Alk* rearrangements in mice injected with both *Eml4* and *Alk* sgRNAs, but not in controls (Figure 2B). The pattern of genomic junctions was similar to those obtained in cells in vitro, with perfect

(E) Examples of chromatograms showing a single base insertion, a microdeletion in the *Alk* intron, and a microdeletion in the *Eml4* intron. Red or blue dashes, deleted bases; green bases, insertions or mutations. Pred., sequence of the predicted genomic junction of *Eml4-Alk* rearrangement.
(F) Detection of *Eml4-Alk* fusion transcripts in ASB-XIV cell line transduced with lentiviral vectors as indicated in (D). RT-PCR shows a fusion transcript between exon13 of *Eml4* and exon 20 of *Alk* genes. Black arrows indicate the position of PCR primers.
(G) An example chromatogram showing the fusion transcripts producing an in-frame EML4-ALK chimeric protein.

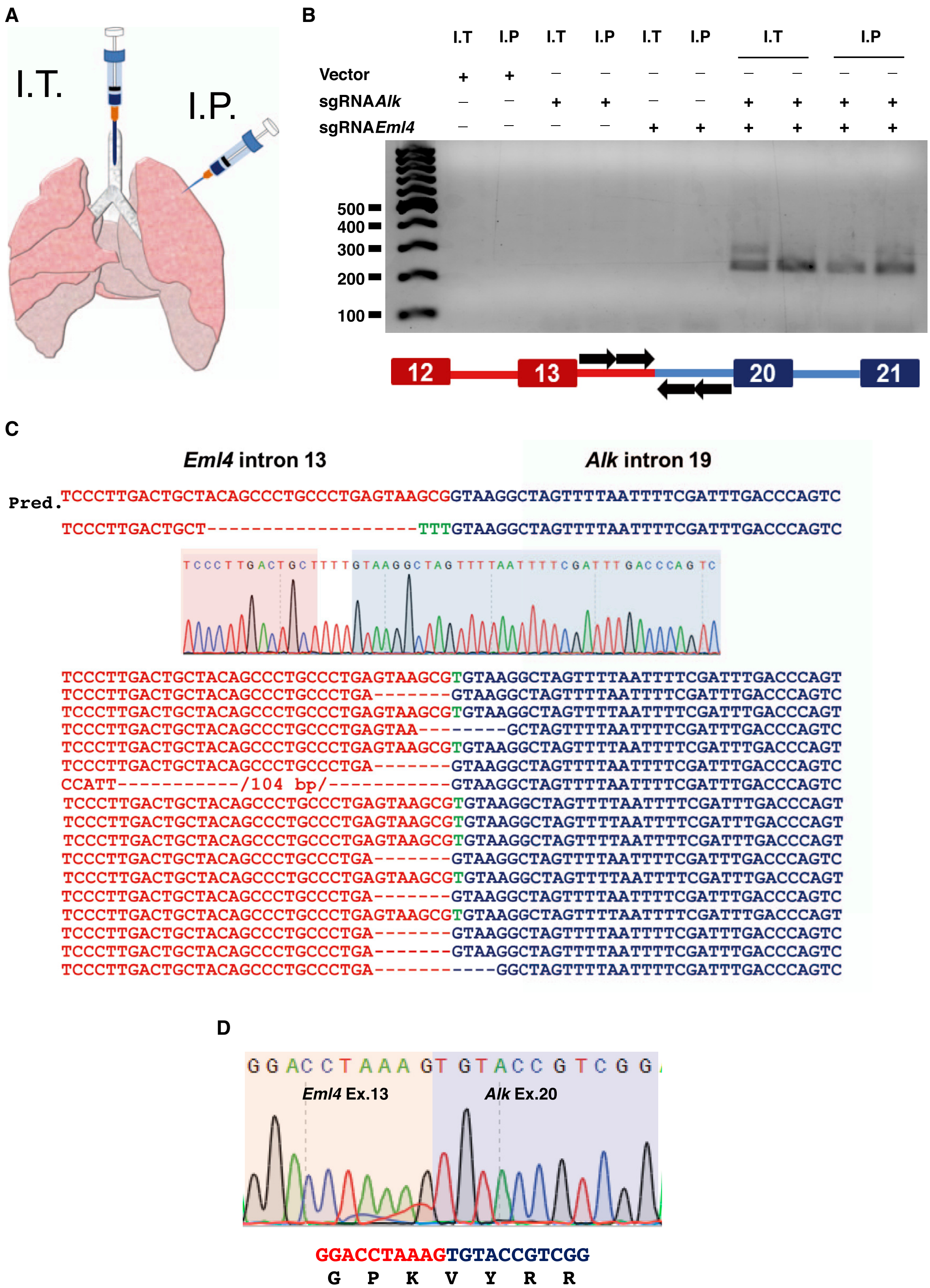

Figure 2. In Vivo Generation of *Eml4-Alk* Rearrangements in Mice

(A) Schematic diagrams showing intratracheal inoculations (I.T.) or intrapulmonary injections (I.P.) of CRISPR/Cas9 lentivirus and isolation of lung epithelial cells.

(legend continued on next page)

junctions or indels (Figure 2C). Remarkably, we also found in vivo genomic junctions corresponding to a 10 Mb deletion or to an interchromosomal translocation between the *Eml4* and *Alk* genomic loci (Figures S3A and S3B). To determine frequency of cells in vivo carrying the genomic *Eml4-Alk* rearrangement, or other genomic events such as 10 Mb deletions, after *Eml4* and *Alk* sgRNA lentiviral infection, we applied a technique previously used to determine the frequency in cell populations of chromosomal translocations such as IgH/c-*myc* in B lymphocytes (Chiarle et al., 2011). By this approach, in four independent mice, we found 17 *Eml4-Alk* rearrangements in 114 independent PCR reactions each from 10^5 cells. All the PCR products were sequenced and confirmed to have the expected genomic *Eml4-Alk* rearrangement. No *Eml4-Alk* rearrangements were found in 152 independent PCR reactions from control mice (i.e., in cells from mice infected with either empty or *Alk* sgRNA-only lentivirus). Thus, we calculated that the frequency of *Eml4-Alk* inversion in vivo was approximately 1.5 rearrangements/10^6 cells for the amount of lentivirus and the technique we used. When we studied the genomic product resulting from the 10 Mb deletion, we found and confirmed by sequencing PCR products corresponding to genomic deletion in 10 out of 38 independent PCR reactions from mice infected with both *Eml4* and *Alk* sgRNAs and in 0 out of 38 controls, giving an estimated frequency of 2.6 deletions/10^6 cells. Finally, by isolating mRNA, we found fusion transcripts coding for an in-frame EML4-ALK chimeric protein as predicted by the genomic breakpoint (Figure 2D). Thus, direct delivery of CRISPR/Cas9 elements to epithelial lung cells can efficiently generate DNA DSBs in vivo that are resolved into chromosomal rearrangements.

Eml4-Alk Inversion Induced by the CRISPR/Cas9 System Drives Tumor Development in Lungs

A critical point was to determine whether the generation of *Eml4-Alk* rearrangements by the CRISPR/Cas9 system was sufficient to drive transformation of lung epithelial cells and therefore lung tumor formation. Transgenic expression of the human EML4-ALK cDNA under either a surfactant protein C (SPC) promoter (Soda et al., 2008) or under a biscistronic CC10-rtTA doxycycline-inducible promoter (Chen et al., 2010) induces the formation of lung tumors. We also developed a GEMM with transgenic expression of human EML4-ALK under the SPC promoter and observed tumor formation with 100% penetrance. Tumor formation was further accelerated by heterozygous or homozygous deletion of *p53* (C.V. and R.C., unpublished data). Therefore, to investigate whether the generation of *Eml4-Alk* rearrangements was sufficient to induce lung tumor formation, we injected CRISPR/Cas9 lentivirus expressing *Eml4* and *Alk* sgRNAs in $p53^{+/-}$ or $p53^{-/-}$ mice. Mice were sacrificed 8 weeks after the injection, and lungs were analyzed for the presence of tumors by histology and immunohistochemistry. We found lung tumors in six out of six $p53^{-/-}$ mice and in four out of four $p53^{+/-}$ mice, but not in control mice (zero out of three $p53^{-/-}$ mice and zero out of three $p53^{+/-}$ mice) (Figure 3A). Tumors were composed of atypical epithelial cells that showed a strong positivity for cytokeratin and a high proliferation index as determined by Ki-67 (Figure 3B). To investigate whether tumor expressed the EML4-ALK fusion protein, we performed immunohistochemistry (IHC) against ALK with an antibody that recognizes the mouse ALK protein. By this approach, we detected positive cells only in tumors from mice infected with *Eml4* and *Alk* sgRNAs, whereas normal lungs in control mice did not show detectable staining (Figure 3C). Next, we wanted to investigate whether such tumors indeed carried the engineered *Eml4-Alk* rearrangement at the genomic DNA. We first used laser capture microdissection (LCM) to dissect tumors and isolate genomic DNA for PCR analysis. As controls, we dissected similarly sized areas of lungs from control mice or from nontumoral areas adjacent to the tumors of mice injected with CRISPR/Cas9 lentivirus expressing *Eml4* and *Alk* sgRNAs. PCR amplification demonstrated the presence of the expected *Eml4-Alk* rearrangements only in the DNA extracted from tumors, but not in both types of controls (Figure 3E). Finally, sequencing of the genomic junction obtained from tumor DNA confirmed the expected *Eml4-Alk* rearrangement generated by DSBs initiated by CRISPR/Cas9 activity (Figure 3F).

DISCUSSION

We have described a simple, fast, and rather inexpensive technique to model oncogenic chromosomal rearrangements directly in adult mice and induce tumor formation. In principle, the CRISPR/Cas9 approach to engineer chromosomal rearrangements could be applied to most, if not all, chromosomal rearrangements as predicted by recent in vitro studies (Choi and Meyerson, 2014; Torres et al., 2014). This technique is embedded with great potential, but we showed that it is also associated with the formation of unwanted genomic rearrangements, such as genomic deletions and, possibly, duplications. Another caveat associated with the CRISPR/Cas9 system is the generation of undesired off-targeting, which appeared as an important concern in original in vitro studies, but it is probably less relevant in vivo (Duan et al., 2014; Hsu et al., 2013; Kuscu et al., 2014; Wu et al., 2014). Thus, all these elements must be carefully considered during the application of such technique to cancer studies.

We expect that this approach could be complementary or even replace time consuming approaches such as traditional knockin targeting of ESCs and lengthy crossing of GEMMs with different genetic backgrounds. Indeed, clear advantages implied by such approach are the possibility of using different cancer-relevant mouse genetic backgrounds for functional studies. To this end, we demonstrated the feasibility of engineering *Eml4-Alk* rearrangements in $p53^{-/-}$ or $p53^{+/-}$ mice, but virtually any viable mouse background could be used. We tested

(B) PCR assay 6 days after lentivirus injections demonstrates that *Eml4-Alk* rearrangements are detectable only in mice injected with CRISPR/Cas9 and *Eml4* and *Alk* sgRNA.

(C) An example chromatogram showing perfect *Eml4-Alk* genomic junction, as well as representative sequences of junctions identified from 17 out of 30 amplicons. Pred., sequence of the predicted genomic junction of *Eml4-Alk* rearrangement.

(D) Representative chromatogram of *Eml4-Alk* fusion transcripts obtained from mRNA extracted from lung cells in vivo.

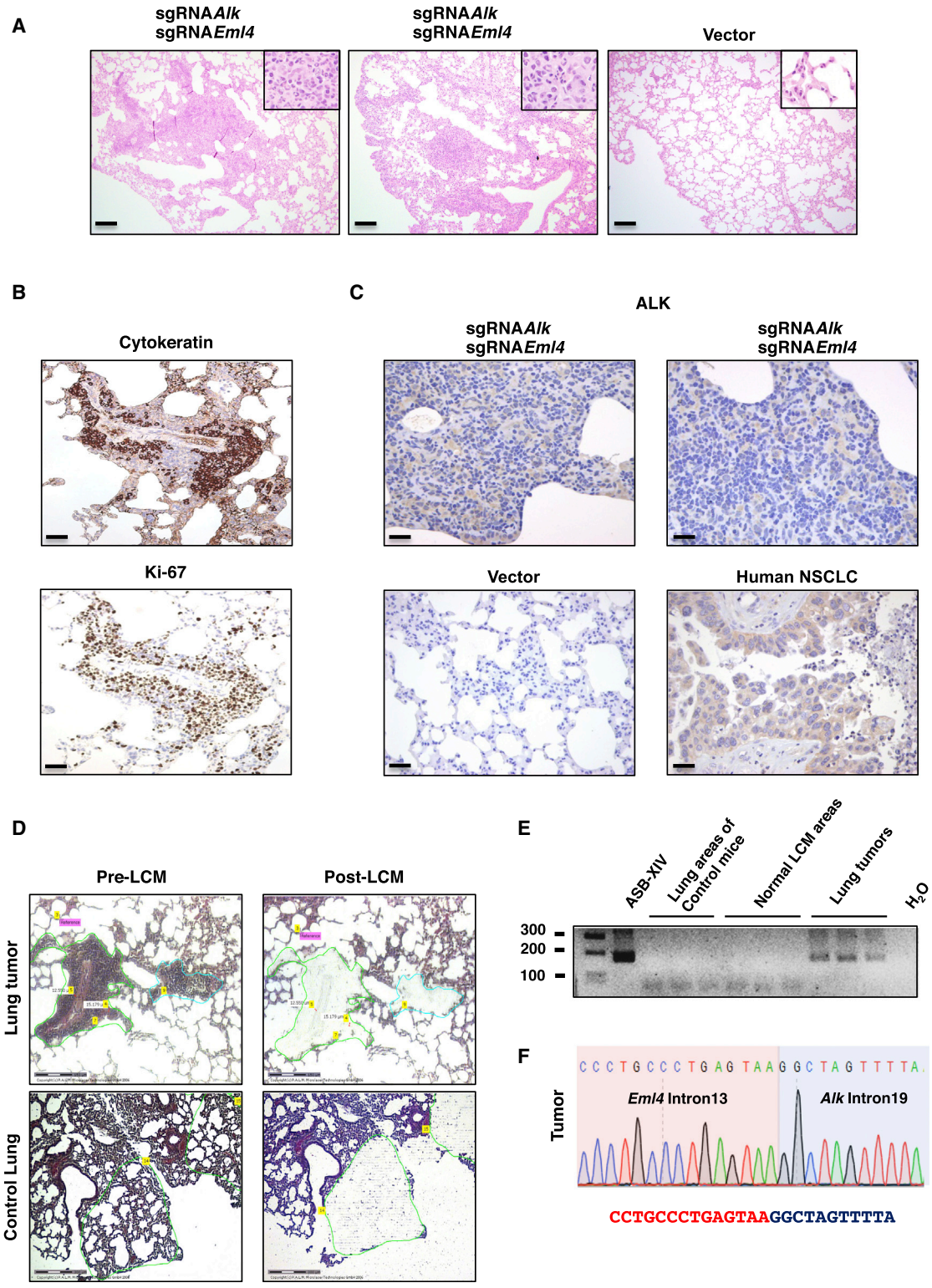

Figure 3. Lung Tumors Generated by CRISPR/Cas9-Induced *Eml4-Alk* Rearrangements

(A) Representative histological sections of lung tumors in $p53^{+/-}$ mice after intrapulmonary injections with two CRISPR/Cas9 lentiviruses expressing the *Eml4* and *Alk* sgRNAs. Control $p53^{+/-}$ mice were injected with a lentiviral vector expressing CRISPR/Cas9, but not sgRNAs. Objective magnification, 10× (inset, 40×). Scale bars represent 100 μm.

(legend continued on next page)

wild-type (WT) mice, but at 8 weeks of age, we could only find small clusters of epithelial hyperplasia, possibly due to the slower tumor development in WT mice as compared to *p53*$^{-/-}$ or *p53*$^{+/-}$ mice. Thus, as compared to *Eml4-Alk* transgenic mice, in our system, CRISPR/Cas9-induced tumors were smaller and less frequent, possibly due to the lower expression levels of the *Eml4-Alk* fusion and the lower frequency of cells carrying the *Eml4-Alk* rearrangement. Recently, it has been shown that expressing both sgRNAs in one single adenoviral vector is efficient in inducing *Eml4-Alk* rearrangements and tumor development (Maddalo et al., 2014).

Additional applications could be envisioned as the possibility of combining several CRISPR/Cas9-mediated targeting for cancer studies. A recent work showed that in the liver of adult mice, the simultaneous disruption of *p53* and PTEN tumor suppressors induced tumor formation (Xue et al., 2014). Therefore, the possibility of combining CRISPR/Cas9-engineered chromosomal rearrangements with multiple targeted gene disruption of oncosuppressors or oncogenes could greatly facilitate and accelerate the study of the complexity of human cancers. The recent generation of a Cre-dependent Cas9 knockin combined with tissue-specific strains of Cre (Platt et al., 2014) could further expand the potential use of the CRISPR/Cas9 system in vivo, as several tissues such as nervous tissues or liver, skin, and bone marrow could be targeted by this technology. To this end, tissue-specific delivery methods to many organs could be easily adapted to the delivery of sgRNAs for the generation of a variety of tissue-specific genomic rearrangements.

EXPERIMENTAL PROCEDURES

Mice

All the animal experiments were approved by the Boston Children's Hospital (BCH) Institutional Animal Care and Use Committee. This review was conducted in accordance with the standards outlined in the National Research Council's *Guide for the Care and Use of Laboratory Animals* and BCH's PHS Assurance.

Cell Culture

Human embryonic kidney 293T (HEK293T) and ASB-XIV cell lines were grown in Dulbecco's modified Eagle's medium (DMEM) supplemented with 10% fetal bovine serum. Primary fibroblast cells were isolated from mouse tail, immortalized with SV40 and maintained in DMEM/Hank's solution.

CRISPR sgRNA Design and Cloning

Alk sgRNA and *Eml4* sgRNA targeted sites were designed manually and checked in silico. Oligomers were annealed and cloned in the BsmBI restriction site of pHKO5 in order to achieve stable expression (Ran et al., 2013). Sequences of *Alk* and *Eml4* sgRNAs are listed in Table S1.

Lentivirus Production and Purification

To produce the lentiviruses, HEK293T cells were seeded at ~70% confluence in 10 cm dishes the day before transfection in D10 media (DMEM supplemented with 10% fetal bovine serum). For each dish, 18 μg of lentiCRISPR plasmid and 3.6 μg of packaging plasmids (pVSV-G, REV, 8.74) were cotransfected into HEK293T cells using a calcium phosphate transfection kit (Clontech) following the manufacturer's recommended protocol. After 30 hr, viruses were harvested and concentrated by ultracentrifugation at 50,000 × *g* for 2 hr at 4°C and resuspended with sterile 1X PBS. Aliquots were stored at −80°C. To evaluate the viral titers, we transduced ASB-XIV or mouse fibroblasts with increasing dilutions of the lentivirus and then selected cells with puromycin, as the lentiviral vectors express the puromycin resistance gene. Even if puromycin selection likely underestimates the number of infectious particles, by counting the numbers of puromycin-resistant cells, we calculated that our lentiviruses contained at least a titer of 1–2 × 10^6/ml infectious particles, with slight variations among different preparations. As we used 40 μl of virus for each mouse inoculation, we estimated that we inoculated 4–8 × 10^4 infectious particles/mouse.

Cell Transduction, Puromycin Selection, and Surveyor Assays

For transduction of fibroblasts or ASB-XIV cells with CRISPR/Cas9 lentivirus, we seeded 2 × 10^4 fibroblasts or 8 × 10^4 ASB-XIV cells into six-well plates. After 24 hr, transduction was performed in fresh media supplemented with 8 μg/ml polybrene (Sigma-Aldrich), and 48 hr later, optimal puromycin concentration was added for selection (6 μg/ml for fibroblasts, 1 μg/ml for ASB-XIV) until noninfected control group cells were completely dead. The SURVEYOR assay was performed as described previously (Cong et al., 2013). Primers used for PCR amplifications are indicated in Table S1.

In Vivo Lentiviral Transduction

Mice were inoculated with lentiviruses either by intratracheal inoculation (Simpson et al., 2001) or by direct intrapulmonary injection (Onn et al., 2003). Briefly, for intratracheal inoculation, a total volume of 40 μl from the different lentiviral combinations was inoculated into 8-week-old BALB/c mice as previously described (Blasco et al., 2011). For intrapulmonary injections, 40 μl volume was injected into the left lobule of 8-week-old mice as previously described (Onn et al., 2003). Mice were sacrificed 6 days after intratracheal inoculations or intrapulmonary injections for molecular studies and 8 weeks after intrapulmonary injections for tumor studies. DNA was obtained from the lungs of these mice following the classical phenol/chloroform extraction.

PCR and RT-PCR for Eml4-Alk Rearrangements

PCR reactions for the different types of genomic rearrangements were performed using DNA from transduced cell lines and lungs as indicated above. Primers used for PCR amplifications are indicated in Table S1. In vivo rearrangements were identified by nested PCR. In a first round of 18 cycles, 1 μg of DNA was used for every reaction. In a second round of 25 cycles, 1 μl of the previous round was used for every reaction. Primers used for PCR amplifications are indicated in Table S1.

For RT-PCR, cDNA synthesis was performed from extracted total RNA and nested PCR was performed for determining the mRNA fusion transcripts originating from the *Eml4-Alk* rearrangement. RT-PCR reactions were sequenced

(B) Immunohistochemical staining for cytokeratin AE1/AE3 (top) and the proliferation marker Ki-67 (bottom) of a representative lung tumor from a *p53*$^{+/-}$ mouse injected with two CRISPR/Cas9 lentiviruses expressing the *Eml4* and *Alk* sgRNAs.
(C) Immunohistochemical staining for ALK in two representative lung tumors from a *p53*$^{+/-}$ mouse injected with two CRISPR/Cas9 lentiviruses expressing the *Eml4* and *Alk* sgRNAs (top), healthy tissue from the same animals (bottom left), and a human ALK-rearranged NSCLC (bottom right).
(D) Representative tumor and healthy lung areas before (left) and after (right) LCM isolation. Scale bars represent 150 μm.
(E) PCR assay on genomic DNA obtained from microdissected normal lung areas of mice injected with control CRISPR/Cas9 lentivirus (Lung areas of Control mice) or nontumoral areas and tumors from mice injected with CRISPR/Cas9 lentiviruses expressing both the *Eml4* and *Alk* sgRNAs (Normal LCM areas and Lung tumors) demonstrates the presence of *Eml4-Alk* rearrangements in lung tumors, but not in control samples. Gel depicts one representative experiment of LCM with three independent tumors out of four independent experiments. DNA from ASB-XIV cells infected with lentiviruses encoding both *Elm4* and *Alk* sgRNAs was used as a positive control for *Eml4-Alk* rearrangement.
(F) An example chromatogram showing an *Eml4-Alk* genomic junction in lung tumors from *Eml4/Alk* sgRNAs CRISPR/Cas9 lentivirus-injected mice.

to confirm the *Eml4-Alk* in frame fusion. Primers used for PCR amplifications are indicated in Table S1.

Immunohistochemistry and LCM

Formalin-fixed paraffin-embedded lung sections were stained with H&E and cytokeratin AE1/AE3 in order to unambiguously detect tumor cells. ALK immunostaining was performed using an anti-ALK rabbit monoclonal antibody (clone sp8, Abcam) and Ki-67 immunostaining with a rabbit monoclonal (clone SP6, Master Diagnostica). The consecutive sections were used for the LCM using a PALMMicroBeam System (Carl Zeiss) controlled with PALM Robosoftware. Approximately 300–500 microdissected cells per region (either tumor cells or normal lung) were captured into caps of 0.5 ml PCR tubes and stored at room temperature. DNA was extracted and processed for nested PCR. Primers used for PCR amplifications are indicated in Table S1.

SUPPLEMENTAL INFORMATION

Supplemental Information includes three figures and one table and can be found with this article online at http://dx.doi.org/10.1016/j.celrep.2014.10.051.

AUTHOR CONTRIBUTIONS

R.B.B. conceived the idea of using CRISPR/Cas9 for *Eml4-Alk* inversion in vivo, performed experiments, prepared the figures, and corrected the manuscript. E.K. provided ideas, performed experiments, and corrected the manuscript. C.A performed the LCM experiment. T.C.C. contributed ideas. E.K., V.G.M., and C.V. helped with experiments. R.C. conceived, supported, and steered the project; provided ideas; and wrote the manuscript.

ACKNOWLEDGMENTS

We thank Feng Zhang and the members of his lab, Le Cong and Neville E. Sanjana, for sharing precious reagents and technical advice. We thank all the members of our lab for discussions and technical help. This work was supported by grants FP7 ERC-2009-StG (proposal 242965, "Lunely"), the Koch Institute-Dana-Farber/Harvard Cancer Center Bridge Project, Associazione Italiana per la Ricerca sul Cancro (AIRC) grant IG-12023, and International Association for Cancer Research (AICR) grant 12-0216. R.B.B. was supported by a fellowship from the Ramon Areces Foundation. C.A. is supported by a fellowship from the Asociación Española Contra el Cáncer (AECC).

Received: September 17, 2014
Revised: October 22, 2014
Accepted: October 24, 2014
Published: November 13, 2014

REFERENCES

Alt, F.W., Zhang, Y., Meng, F.L., Guo, C., and Schwer, B. (2013). Mechanisms of programmed DNA lesions and genomic instability in the immune system. Cell *152*, 417–429.

Blasco, R.B., Francoz, S., Santamaría, D., Cañamero, M., Dubus, P., Charron, J., Baccarini, M., and Barbacid, M. (2011). c-Raf, but not B-Raf, is essential for development of K-Ras oncogene-driven non-small cell lung carcinoma. Cancer Cell *19*, 652–663.

Boboila, C., Alt, F.W., and Schwer, B. (2012). Classical and alternative end-joining pathways for repair of lymphocyte-specific and general DNA double-strand breaks. Adv. Immunol. *116*, 1–49.

Brunet, E., Simsek, D., Tomishima, M., DeKelver, R., Choi, V.M., Gregory, P., Urnov, F., Weinstock, D.M., and Jasin, M. (2009). Chromosomal translocations induced at specified loci in human stem cells. Proc. Natl. Acad. Sci. USA *106*, 10620–10625.

Chen, Z., Sasaki, T., Tan, X., Carretero, J., Shimamura, T., Li, D., Xu, C., Wang, Y., Adelmant, G.O., Capelletti, M., et al. (2010). Inhibition of ALK, PI3K/MEK, and HSP90 in murine lung adenocarcinoma induced by EML4-ALK fusion oncogene. Cancer Res. *70*, 9827–9836.

Chiarle, R., Voena, C., Ambrogio, C., Piva, R., and Inghirami, G. (2008). The anaplastic lymphoma kinase in the pathogenesis of cancer. Nat. Rev. Cancer *8*, 11–23.

Chiarle, R., Zhang, Y., Frock, R.L., Lewis, S.M., Molinie, B., Ho, Y.J., Myers, D.R., Choi, V.W., Compagno, M., Malkin, D.J., et al. (2011). Genome-wide translocation sequencing reveals mechanisms of chromosome breaks and rearrangements in B cells. Cell *147*, 107–119.

Choi, P.S., and Meyerson, M. (2014). Targeted genomic rearrangements using CRISPR/Cas technology. Nat Commun *5*, 3728.

Cong, L., Ran, F.A., Cox, D., Lin, S., Barretto, R., Habib, N., Hsu, P.D., Wu, X., Jiang, W., Marraffini, L.A., and Zhang, F. (2013). Multiplex genome engineering using CRISPR/Cas systems. Science *339*, 819–823.

Duan, J., Lu, G., Xie, Z., Lou, M., Luo, J., Guo, L., and Zhang, Y. (2014). Genome-wide identification of CRISPR/Cas9 off-targets in human genome. Cell Res. *24*, 1009–1012.

Gilbert, L.A., Larson, M.H., Morsut, L., Liu, Z., Brar, G.A., Torres, S.E., Stern-Ginossar, N., Brandman, O., Whitehead, E.H., Doudna, J.A., et al. (2013). CRISPR-mediated modular RNA-guided regulation of transcription in eukaryotes. Cell *154*, 442–451.

Gostissa, M., Alt, F.W., and Chiarle, R. (2011). Mechanisms that promote and suppress chromosomal translocations in lymphocytes. Annu. Rev. Immunol. *29*, 319–350.

Gostissa, M., Schwer, B., Chang, A., Dong, J., Meyers, R.M., Marecki, G.T., Choi, V.W., Chiarle, R., Zarrin, A.A., and Alt, F.W. (2014). IgH class switching exploits a general property of two DNA breaks to be joined incis over long chromosomal distances. Proc. Natl. Acad. Sci. USA *111*, 2644–2649.

Gupta, A., Hall, V.L., Kok, F.O., Shin, M., McNulty, J.C., Lawson, N.D., and Wolfe, S.A. (2013). Targeted chromosomal deletions and inversions in zebrafish. Genome Res. *23*, 1008–1017.

Hakim, O., Resch, W., Yamane, A., Klein, I., Kieffer-Kwon, K.R., Jankovic, M., Oliveira, T., Bothmer, A., Voss, T.C., Ansarah-Sobrinho, C., et al. (2012). DNA damage defines sites of recurrent chromosomal translocations in B lymphocytes. Nature *484*, 69–74.

Hsu, P.D., Scott, D.A., Weinstein, J.A., Ran, F.A., Konermann, S., Agarwala, V., Li, Y., Fine, E.J., Wu, X., Shalem, O., et al. (2013). DNA targeting specificity of RNA-guided Cas9 nucleases. Nat. Biotechnol. *31*, 827–832.

Jao, L.E., Wente, S.R., and Chen, W. (2013). Efficient multiplex biallelic zebrafish genome editing using a CRISPR nuclease system. Proc. Natl. Acad. Sci. USA *110*, 13904–13909.

Klein, I.A., Resch, W., Jankovic, M., Oliveira, T., Yamane, A., Nakahashi, H., Di Virgilio, M., Bothmer, A., Nussenzweig, A., Robbiani, D.F., et al. (2011). Translocation-capture sequencing reveals the extent and nature of chromosomal rearrangements in B lymphocytes. Cell *147*, 95–106.

Kuscu, C., Arslan, S., Singh, R., Thorpe, J., and Adli, M. (2014). Genome-wide analysis reveals characteristics of off-target sites bound by the Cas9 endonuclease. Nat. Biotechnol. *32*, 677–683.

Lee, H.J., Kweon, J., Kim, E., Kim, S., and Kim, J.S. (2012). Targeted chromosomal duplications and inversions in the human genome using zinc finger nucleases. Genome Res. *22*, 539–548.

Long, C., McAnally, J.R., Shelton, J.M., Mireault, A.A., Bassel-Duby, R., and Olson, E.N. (2014). Prevention of muscular dystrophy in mice by CRISPR/Cas9-mediated editing of germline DNA. Science *345*, 1184–1188.

Maddalo, D., Manchado, E., Concepcion, C.P., Bonetti, C., Vidigal, J.A., Han, Y.C., Ogrodowski, P., Crippa, A., Rekhtman, N., de Stanchina, E., et al. (2014). In vivo engineering of oncogenic chromosomal rearrangements with the CRISPR/Cas9 system. Nature, Published online October 22, 2014. http://dx.doi.org/10.1038/nature13902.

Mali, P., Yang, L., Esvelt, K.M., Aach, J., Guell, M., DiCarlo, J.E., Norville, J.E., and Church, G.M. (2013). RNA-guided human genome engineering via Cas9. Science *339*, 823–826.

Mano, H. (2008). Non-solid oncogenes in solid tumors: EML4-ALK fusion genes in lung cancer. Cancer Sci. *99*, 2349–2355.

Mitelman, F., Johansson, B., and Mertens, F. (2007). The impact of translocations and gene fusions on cancer causation. Nat. Rev. Cancer *7*, 233–245.

Onn, A., Isobe, T., Itasaka, S., Wu, W., O'Reilly, M.S., Ki Hong, W., Fidler, I.J., and Herbst, R.S. (2003). Development of an orthotopic model to study the biology and therapy of primary human lung cancer in nude mice. Clin. Cancer Res. *9*, 5532–5539.

Piganeau, M., Ghezraoui, H., De Cian, A., Guittat, L., Tomishima, M., Perrouault, L., René, O., Katibah, G.E., Zhang, L., Holmes, M.C., et al. (2013). Cancer translocations in human cells induced by zinc finger and TALE nucleases. Genome Res. *23*, 1182–1193.

Platt, R.J., Chen, S., Zhou, Y., Yim, M.J., Swiech, L., Kempton, H.R., Dahlman, J.E., Parnas, O., Eisenhaure, T.M., Jovanovic, M., et al. (2014). CRISPR-Cas9 Knockin Mice for Genome Editing and Cancer Modeling. Cell *159*, 440–455.

Rabbitts, T.H., Appert, A., Chung, G., Collins, E.C., Drynan, L., Forster, A., Lobato, M.N., McCormack, M.P., Pannell, R., Spandidos, A., et al. (2001). Mouse models of human chromosomal translocations and approaches to cancer therapy. Blood Cells Mol. Dis. *27*, 249–259.

Ran, F.A., Hsu, P.D., Wright, J., Agarwala, V., Scott, D.A., and Zhang, F. (2013). Genome engineering using the CRISPR-Cas9 system. Nat. Protoc. *8*, 2281–2308.

Shaw, A.T., and Engelman, J.A. (2013). ALK in lung cancer: past, present, and future. J. Clin. Oncol. *31*, 1105–1111.

Simpson, A.J., Wallace, W.A., Marsden, M.E., Govan, J.R., Porteous, D.J., Haslett, C., and Sallenave, J.M. (2001). Adenoviral augmentation of elafin protects the lung against acute injury mediated by activated neutrophils and bacterial infection. J. Immunol. *167*, 1778–1786.

Soda, M., Choi, Y.L., Enomoto, M., Takada, S., Yamashita, Y., Ishikawa, S., Fujiwara, S., Watanabe, H., Kurashina, K., Hatanaka, H., et al. (2007). Identification of the transforming EML4-ALK fusion gene in non-small-cell lung cancer. Nature *448*, 561–566.

Soda, M., Takada, S., Takeuchi, K., Choi, Y.L., Enomoto, M., Ueno, T., Haruta, H., Hamada, T., Yamashita, Y., Ishikawa, Y., et al. (2008). A mouse model for EML4-ALK-positive lung cancer. Proc. Natl. Acad. Sci. USA *105*, 19893–19897.

Torres, R., Martin, M.C., Garcia, A., Cigudosa, J.C., Ramirez, J.C., and Rodriguez-Perales, S. (2014). Engineering human tumour-associated chromosomal translocations with the RNA-guided CRISPR-Cas9 system. Nat Commun *5*, 3964.

Wang, H., Yang, H., Shivalila, C.S., Dawlaty, M.M., Cheng, A.W., Zhang, F., and Jaenisch, R. (2013). One-step generation of mice carrying mutations in multiple genes by CRISPR/Cas-mediated genome engineering. Cell *153*, 910–918.

Wu, X., Scott, D.A., Kriz, A.J., Chiu, A.C., Hsu, P.D., Dadon, D.B., Cheng, A.W., Trevino, A.E., Konermann, S., Chen, S., et al. (2014). Genome-wide binding of the CRISPR endonuclease Cas9 in mammalian cells. Nat. Biotechnol. *32*, 670–676.

Xiao, A., Wang, Z., Hu, Y., Wu, Y., Luo, Z., Yang, Z., Zu, Y., Li, W., Huang, P., Tong, X., et al. (2013). Chromosomal deletions and inversions mediated by TALENs and CRISPR/Cas in zebrafish. Nucleic Acids Res. *41*, e141.

Xue, W., Chen, S., Yin, H., Tammela, T., Papagiannakopoulos, T., Joshi, N.S., Cai, W., Yang, G., Bronson, R., Crowley, D.G., et al. (2014). CRISPR-mediated direct mutation of cancer genes in the mouse liver. Nature *514*, 380–384.

Yang, H., Wang, H., Shivalila, C.S., Cheng, A.W., Shi, L., and Jaenisch, R. (2013). One-step generation of mice carrying reporter and conditional alleles by CRISPR/Cas-mediated genome engineering. Cell *154*, 1370–1379.

Yin, H., Xue, W., Chen, S., Bogorad, R.L., Benedetti, E., Grompe, M., Koteliansky, V., Sharp, P.A., Jacks, T., and Anderson, D.G. (2014). Genome editing with Cas9 in adult mice corrects a disease mutation and phenotype. Nat. Biotechnol. *32*, 551–553.

Zarrin, A.A., Del Vecchio, C., Tseng, E., Gleason, M., Zarin, P., Tian, M., and Alt, F.W. (2007). Antibody class switching mediated by yeast endonuclease-generated DNA breaks. Science *315*, 377–381.

Zhang, Y., McCord, R.P., Ho, Y.J., Lajoie, B.R., Hildebrand, D.G., Simon, A.C., Becker, M.S., Alt, F.W., and Dekker, J. (2012). Spatial organization of the mouse genome and its role in recurrent chromosomal translocations. Cell *148*, 908–921.